Chapter 2
Energy Harvesting Electronic Systems

Abstract This chapter presents a literature review about the various ambient energy sources that can be harvested and the description of some related systems. As such, this chapter will provide a brief overview about each source and describe some systems that use that same energy source. This will be extended on to the domain of the wireless sensor networks and the aspects related to it, being presented some examples of energy harvesting powered WSN in different environments. A brief description of what is expected from each network and how it succeeds in harvesting the energy that enables it to work will receive a particular focus. Since light is the energy source being harvested, in order to power the system described in this book, some more attention will be dedicated to the analysis of this source. Proceeding with this purpose, a more detailed overview about PV technologies will be given in Chap. 3. In addition, a more focused insight covering DC–DC converters, energy storing devices, and MPPT techniques will be given in Chap. 4, so as to complete the literature review opened up in the present chapter.

2.1 Available Energy Sources

In the surrounding environment, there are a number of possible energy sources that can be conveniently harvested, in order to power electronic applications [1]. Depending on whether a certain energy source is more abundant, that could be the preferred one.

However, another possible configuration that performs ambient energy scavenging relies on the conjunction of multiple energy sources, like in [1–7]. The latter is a highly miniaturized system, designed to have modularity, in the sense that one can add or remove IC layers, which communicate among themselves using the I^2C protocol. This system occupies a volume of only 1 mm^3, entering in the category of smart dust, which are wireless sensor nodes with perpetual energy harvesting. Next, Fig. 2.1 shows the evolution in terms of volume reduction that occurred over the past decades, in conformity with Bell's law, as stated in [7]. This law is somewhat related to the well-known Moore's law [8], although the latter may probably be reaching its limit [9].

C.M. Ferreira Carvalho and N.F.S.V. Paulino, *CMOS Indoor Light Energy Harvesting System for Wireless Sensing Applications*,
DOI 10.1007/978-3-319-21617-1_2

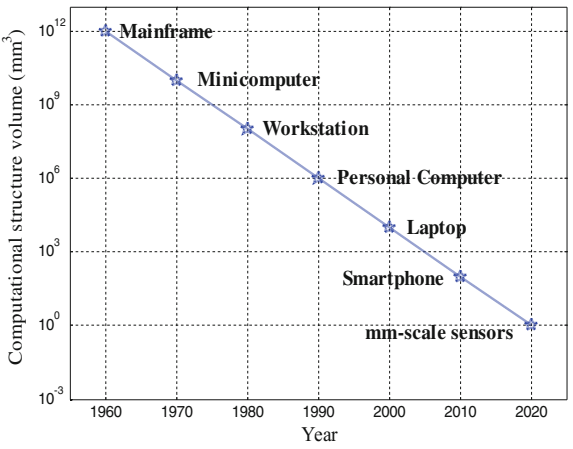

Fig. 2.1 Continuous downscaling of micro-size computing systems

The scavenged energy sources more commonly used are presented in this chapter and very briefly described and characterized in the following subsections, as a more detailed overview is outside the scope of this book. However, relevant references will be given, in order to aid in getting a broader insight about each source and related systems that are specifically designed to work with it.

2.1.1 Mechanical Energy

Mechanical energy can be harvested from various natural sources, such as wind [10], wave motion [11], vehicle motion, or in general, any kind of vibrations or movement, namely by resonance. There is an important issue specific to mechanical energy harvesting systems, which is the need to have rectifying circuits. As one is dealing with alternating signals, an AC to DC conversion must be carried out. The rectifiers can be passive or active. The former ones are based on diode topologies, namely rectifier bridges, while the latter ones employ some means of switching power conversion, as in [12].

There are several ways of converting mechanical energy into electrical energy, from which one can choose. This conversion can be done by using electromagnetic [1, 13], piezoelectric [14], or electrostatic means [15]. According to [13], the most suitable materials to harvest mechanical energy are those that exploit the electromagnetic and the piezoelectric principles, possessing the highest power density, when compared to the electrostatic ones. Each of these materials has a different electrical behavior, and thus, when using any of them, a different electric interface must be used. Harvesters exploiting vibrations presently have an efficiency ranging from 25 to 50 % [16].

2.1.1.1 Electromagnetic Conversion

In order to have the possibility to perform simulations, destinated to check any proof of concept, it is necessary to have a model of the harvester device. In the mechanical context, when dealing with electromagnetic conversion devices, it is usual to have finite element method (FEM) models, so as to have a suitable representation of the harvester. This model can be used in conjunction with electric circuits, in order to enable a simulation. For example, in [13], an electromagnetic energy harvester is studied using this approach. From the FEM model, one can extrapolate a block diagram model at the numerical level and this one can then be translated to Spectre, for example, allowing for electric simulation. In the block diagram model, one will have the kinematic variables playing their role.

Electromagnetic transducers generate a voltage offering a low impedance output, and typically, electromagnetic conversion is used for larger power levels than the ones aimed by this book, and, therefore, it will not be addressed further. Moreover, the cost of this type of converters is higher than that for other types.

2.1.1.2 Piezoelectric Conversion

There is a material, Lead Zirconium Titanate (PZT), widely used for this conversion, which is considered as the silicon counterpart of piezoelectric materials, when dealing with engineering applications, as it can be found in [6, 17, 18].

A piezoelectric energy harvester is typically a cantilevered beam with one or two piezoceramic layers, which can vibrate in various vibration modes. The induced strain is converted into electrical charge, originating a voltage. The generated voltage is proportional to the force and thus to the vibration magnitude applied to the harvester. However, piezoelectric energy transducers are characterized by a high impedance output, unlike conventional voltage sources. This results in the need to use appropriate electric circuits that correctly interface with this type of transducer. The voltage generation mechanism is illustrated in Fig. 2.2.

This kind of mechanism is bidirectional, such that by applying a voltage will result in a deformation, meaning that these materials can be used both as sensors and as actuators.

The simplified electric model of a unimodal piezoelectric harvester is represented in Fig. 2.3a.

At the left-hand side of Fig. 2.3a, the mechanical part of the model is represented, where R, L, and C represent the mechanical parameter loss, mass, and stiffness, respectively. The transition from the mechanical to the electrical domain is modeled by a transformer with a ratio of n, where the conversion from stiffness to the current i is performed, instead of using the generated voltage directly. At the right-hand side, i.e., in the electrical domain, C_p represents the plate capacitance of the piezoelectric material. When at resonance, the whole circuit can be simplified to a current source in parallel with a capacitor and a resistor, in which the latter represents the losses. This model is depicted in Fig. 2.3b. With this circuit, the MPP

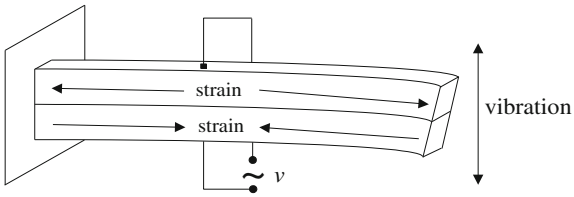

Fig. 2.2 Voltage generation mechanism in a piezoelectric harvester

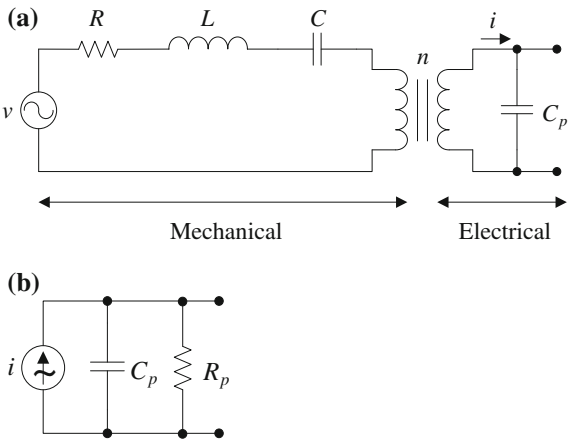

Fig. 2.3 Simplified model of the piezoelectric harvester (according to [19])

condition can be achieved if the load connected at the output is the conjugate of the impedance represented by C_p and R_p, i.e., the load must have an inductive component.

2.1.1.3 Electrostatic Conversion

Micro-electrical mechanical systems (MEMS) are well suited to collect mechanical energy. Devices using this kind of technology can be built so as to be compatible with CMOS integration, in order to lay out both the harvester and the energy processing system in the same die.

Basically, the harvester can consist of a simple variable plate-distance capacitor. The energy conversion can be achieved in two ways, either by varying the gap between the plates or by varying their overlap. A simple way to illustrate this principle is by looking at Fig. 2.4, representing a rest position, from where the moving plate can suffer a translation along any of the axis, as a consequence of vibrations or any other motion.

If this translation occurs along the *y*-axis, the distance between plates will vary, and the capacitance will vary accordingly, in an inversely proportional way. On the other hand, if the translation occurs along the *x*- or the *z*-axis, the plate overlap will

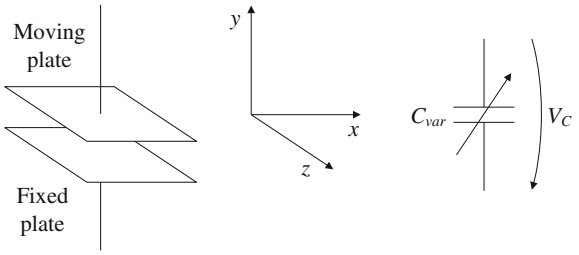

Fig. 2.4 Symbolic representation of the conversion mechanism using MEMS

decrease and so will the resulting capacitance. If the capacitor is precharged and then kept open-circuited with a constant charge, the capacitance variation will change the voltage of the capacitor (V_C) and, consequently, the stored energy [20].

The variation of capacitance is given by the parallel plate capacitor equation,

$$C_{\text{var}} = \varepsilon_0 \varepsilon_r \frac{A}{d}, \tag{2.1}$$

and relies on modifying either the superposition area of the plates of the capacitor (A), the distance between plates (d), or even the dielectric constant of the insulation material between plates (ε_r), if a different material is inserted in between. ε_0 is the dielectric constant of vacuum.

By having established the value for the variable capacitance, the voltage that appears at the terminals of the capacitor is

$$V_C = \frac{Q}{C_{\text{var}}}, \tag{2.2}$$

and the energy that can be used thanks to this generation process, if the capacitor is discharged over a resistor R during an interval t_{on}, is

$$E(t) = \int_0^{t_{\text{on}}} \frac{V_C^2}{R} e^{-\frac{2t}{RC_{\text{var}}}} dt. \tag{2.3}$$

MEMS are also compatible with both the piezoelectric and electromagnetic processes.

2.1.2 Thermal Gradients

Obtaining energy from temperature sources may be an option in certain contexts, for instance, where there are high temperatures, such as furnaces or exhaust pipes.

These can be conveniently scavenged as a thermal source, providing a consistent amount of power [1, 3, 17, 18].

Thermoelectric generators (TEG) have the advantageous characteristics of requiring little or none amount of human intervention during their useful lifetime. Moreover, these devices are reliable and quiet, as there are no moving parts.

Current thermoelectric materials can only convert a maximum of 5–6 % of the useful heat into electricity. However, significant research is being carried out, in order to develop new materials and module constructions which can eventually reach a harvesting efficiency higher than 10 % [21].

A thermoelectric element converts thermal energy, in the form of temperature differences, into electrical energy and vice versa. Devices using Bi_2Te_3 have already proven their usefulness [18] and showed to possess the highest figure of merit [22], defined as

$$Z \cdot T = \frac{\alpha^2 \sigma}{\lambda} \cdot T, \tag{2.4}$$

in which, T is the temperature, α is the Seebeck coefficient, σ is the electrical resistivity, and λ is thermal conductivity. Using this material, for temperatures between −50 and 80 °C, the figure of merit in (2.4) can reach values up to unity.

The drawback behind this kind of source comes from the hostile environment to be scavenged, having to take particular care with the electronic circuits being powered. Thermopiles are among the other types of devices to achieve harvesting from this kind of source, but there are also some novel devices and systems under research [17, 23].

The model of a thermoelectric energy harvester is a simple Thévenin equivalent circuit, like the one shown in Fig. 2.5.

The voltage V_T is an open-circuit voltage proportional to the temperature difference between both sides of the TEG, and to the Seebeck coefficient. The latter depends on the material being used and represents a measure of the magnitude of an induced thermoelectric voltage, in response to a temperature difference across that same material. In the model of Fig. 2.5, resistance R_T represents the loss of the model of the TEG and V_{TH} is the output voltage of the harvester. According to the maximum power transfer theorem, the maximum power point can be achieved by matching a load resistance to the source resistance, R_T.

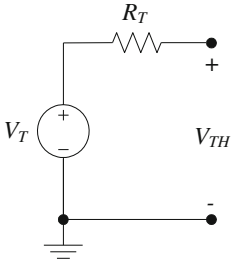

Fig. 2.5 Electrical equivalent of the thermoelectric generator

The Seebeck effect is the generation of an electromotive force within two different metals, when their junctions are maintained at different temperatures. A common application of this principle is the use of thermocouples to measure temperature. However, when a thermocouple is used in temperature measurements, the electromotive force being generated is countered by an applied voltage, resulting in no current flowing. The main difference, between using the thermoelectric effect for temperature measurement or for power generation, is the use of semiconductor materials, instead of metals, when the purpose is the latter. This use enables the flow of current in the generator, allowing it to produce power.

The Seebeck coefficient is defined as the obtained voltage variation in response to each degree of temperature gradient. Thus, the thermoelectrically generated voltage in the model of Fig. 2.5 (V_T) is given by (2.5), where S is the Seebeck coefficient (expressed in V/K), which is material-dependent, and ΔT is the temperature difference between the hot and the cold sides of the harvester device.

$$V_T = S\Delta T. \tag{2.5}$$

Semiconductor materials have a significantly higher Seebeck coefficient, when compared to metals, and so they are more suited to manufacture power generator devices. The Seebeck effect in the n-type material creates a flow of excess electrons from the hot junction to the cold one. In the p-type material, holes migrate toward the cold side creating a net current flow which is in the same direction as the one in the n-type material. In Fig. 2.6, the simplified schematic structure of a typical semiconductor thermoelectric device is shown.

MEMS structures are also used for building TEG, and, in [24], a new MEMS fabrication method is presented.

For example, a WSN able to monitor the health of the structure of an aircraft can be established [22]. One of the main advantages of a WSN is to avoid complex wiring, saving material, and consequently weight and cost. The temperature difference obtained between the aircraft cabin and the aircraft body shell, at high altitudes, can be such to obtain a high potential.

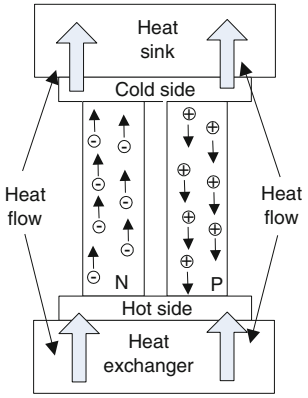

Fig. 2.6 Typical structure of a semiconductor thermoelectric harvester

At a bigger scale, thinking about renewable energy sources and environmental issues, [25] proposes using ocean thermal energy conversion (OTEC), by taking advantage of the difference of about 20 °C existing in subzero regions. Since the water is almost at freezing level, and the outside temperature can be at about −20 °C, this permanent temperature gradient is suitable for thermal energy harvesting. At a smaller scale, this factor could be interesting to deploy a WSN in these geographical zones of the ocean, with the nodes being supplied by this harvestable source.

There are also environments at a much smaller scale, such as wireless body area networks (WBAN), which can also make use of thermal gradients, by using human warmth. This topic will be further explored in Sect. 2.1.4.

More recently, new technologies have been developed by using an innovative concept of mixing mechanical and thermal energy to harvest energy. This is done by firstly using heat to provoke a deformation in a material, such as a bimetallic. Secondly, that deformation, by electrostatic conversion (see Sect. 2.1.1.3), is used to produce energy. Such developments can be found in [26, 27].

2.1.3 Radio Frequency Electromagnetic Energy

In environments mostly located in urban areas, one source that becomes appealing to be harvested is the radio frequency (RF) energy. This energy exists around every place and is generated by sources such as radio and television broadcasting, mobile phone cellular network, Wi-Fi networks, and other sources alike.

One important factor that makes this source very appealing to harvest is the fact that ambient RF energy, as a power source for outdoor sensor nodes, is typically available all the time, either day or night.

As the harvested signals are AC, in order to provide at the end of the chain a stable DC supply, it is necessary to use rectifiers to perform such a conditioning, like it can be found in [3, 6, 28]. Harvesters exploiting the RF sources presently have an efficiency that can go up to 50 % [16].

The low magnitude of the voltages resulting from the RF energy harvesting process is at such reduced level that the design of rectifiers is very challenging, since many half-wave or full-wave diode rectifiers require nonzero turn-on voltages to operate.

Typical rectifier circuits are based on the well-known diode bridge. These can make use of NMOS or PMOS transistors and can implement half- or full-wave rectifiers. According to design parameters and required performance, some trade-offs must be adopted.

In Fig. 2.7, a way of implementing a MOSFET rectifier circuit using NMOS devices is shown [6]. Voltage v_{in} represents the RF source being harvested.

The rectifying process is as follows: When v_{in} is in its positive half cycle, M_1 and M_4 are conducting current, while M_2 and M_3 are in open circuit. During the negative half cycle of v_{in}, the roles of the transistors are exchanged. At the end, the rectified

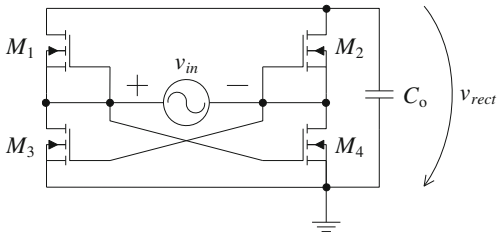

Fig. 2.7 NMOS full-wave rectifier

voltage v_{rect} will ideally be a DC voltage, appearing at the terminals of the filtering capacitor C_{o}.

With circuits like the one shown, a low voltage drop (v_{ds}) in the transistors implies using wide channels and low frequencies. On the opposite, narrow channels imply a higher voltage drop and the operation at higher frequencies. If, instead of just one transistor, several transistors are connected in parallel, the performance of the rectifier can be improved in terms of working frequency and voltage drop. This technique divides the total current by each one of the transistors in the parallel, thus reducing the voltage drop of each individual device. In addition, frequency can also be improved, because the size of each transistor is smaller, as compared to having just one big transistor. In [6], the implementation of full-wave rectifiers allowed to obtain voltage drops as low as 0.2 V and operating frequencies of 16 MHz, by using a parallel structure of transistors with $W = 10$ μm and $L = 0.28$ μm.

In [28], a different type of rectifier is used, by making a field-to-voltage conversion, which is not grounded. This structure is depicted in Fig. 2.8, where $v_{\text{in}-}$ and $v_{\text{in}+}$ connect to an antenna or similar device.

The v_{REF} terminal allows for offsetting the output voltage v_{out}. Using this structure, it is possible to stack several of these modules, in which the lower one can have v_{REF} grounded, while its output terminal connects to the v_{REF} terminal of the next structure, and so on. By doing so, the contribution of each rectifier helps to effectively increase the overall output voltage, so as to have, at the output of the upper structure, a suitable value to power an electronic application. A more detailed

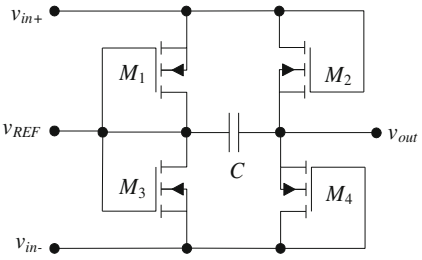

Fig. 2.8 Full-wave rectifier, acting as a field-to-voltage converter

study of MOSFET rectifiers is done in [29], where the transistors are working in the weak inversion region, having all of the terminals being exploited.

This RF energy source appears typically in a very limited amount, representing a very low power density [17]. In order to assess the real availability of energy that could be made useful by using RF sources, by performing power density measurements, [30] surveys the expected power density levels from GSM 900 and GSM 1800 base stations at a certain distance and also in a WLAN environment. According to it, for distances ranging from 25 to 100 m from a GSM base station, power density levels range from 0.1 to 3.0 mW/m^2. Measurements in a WLAN environment indicated even lower power density values, thus making GSM and WLAN unlikely to produce enough ambient RF energy for wirelessly powering miniature sensors. Also according to [30], a single GSM telephone has proven to deliver enough energy for wirelessly powering small applications at moderate distances.

In general, the levels of power density are much dependent on the frequency of operation and on the distance between the transmitter base station and the receiving harvester.

At a bigger scale, thinking about grid power transfer, [31] presents some results about wireless power transfer, although at reduced distances, as electromagnetic energy has a strong decay over distance and with the frequency being used.

An essential part of this kind of system is the antenna, in order to capture the radio signals. There is a system that agglutinates the functionality of antenna and rectifier, which is called a rectenna. These devices, and antennas in general, have a relatively low conversion efficiency, but this parameter is dependent on the frequency of operation. As such, the key parameters to have into consideration are bandwidth, polarization, directivity, and size. In order to be sensitive to a wider range of frequencies, the antenna must tend to be bigger, in order to capture the lower frequencies. The work in [32] presents an architecture for a RF energy harvesting system, where the system components such as the antenna and the ultra-wideband (UWB) input matching *LC* network are designed and studied in depth, as well as the optimum rectenna load. Also, a study about the availability of RF ambient energy, coming from digital television broadcasting in a given geographical area and its surroundings, is carried out in [32].

The work developed in [33], besides making use of television broadcasting, also uses the energy radiated by the base transceiver stations of the mobile telephone networks. The collected energy is sufficient to power a sensing application, whose objective is to transmit information about temperature and light. The duty cycle being used is very small, and the firmware is implemented with particular care about reducing computationally consuming operations.

The applications described in [3, 6] make use of radio frequency (RF) power as a resource to be harvested in conjunction with other sources. However, in [28, 32, 33], this is the only source being scavenged.

Another important set of applications that make use of RF energy harvesting is the radio frequency identification (RFID) tags, widely disseminated in commercially available consumer products. When queried by a reader device, the tag is

momentarily powered by a RF signal close to it and responds by sending a coded identification number. The same type of device can also be used to identify livestock or pets, in which the tag is implanted beneath the skin.

To harvest the electromagnetic energy in RFID systems, an antenna or an inductor coil must be used. However, as with other sources, this RF energy may present itself unpredictable and much dependent on the distance at which the reader is put from the tag. In [34], a system is presented in order to enhance range operation. Due to the dependence on the distance between the reader and the tag, voltage limiter circuits must be used to prevent any damage to the tag being read. Examples of limiter architectures with such a purpose are presented in [35, 36].

2.1.4 Human Generation

The idea behind using applications powered by a human source is very interesting and has captivated the interest of researchers since some years ago [37]. The human body provides multiple sources of energy that can be harvested. According to [38], it has been shown that, ideally, 2.4–4.8 W of power is available in body heat, 0.4 W in exhalation, 0.37 W in blood pressure, 0.76–2.1 mW in finger motion, 60 W in arm motion, 67 W in heel strike, 69.8 W in ankle motion, 49.5 W in knee motion, 39.2 W in hip motion, 2.1 W in elbow motion, and 2.2 W in shoulder motion.

The necessity of providing energy to wearable computing devices made the conversion of human motion into useful electrical energy, a topic of extensive study. For instance, in gyms, there is some equipment, such as exercising bicycles that have their instrument panel powered by the user who is exercising. However, in such a situation, the user must strive forcefully into the production of the required energy. More broadly, in energy harvesting generated by human motion, the preferable situation is to have the user oblivious of such an action, while providing the necessary energy to power an electronic application. For example, the kinetic energy from human motion is already used to power electronic wrist watches [39]. In the medical domain, electronic medical implants can be powered by using the human heat as a power source.

In fact, the energy generated by human means is coming from a particular environment where there coexist some of the sources already described, namely the thermal gradients and the mechanical energy sources, but that are not restricted to these. Energy harvesting of electromagnetic radiations is also possible with the human body, as it will be shown ahead.

A very important class of applications, in a human energy harvesting environment, is the implantable biosensor. There are some requirements for these sensor systems, which are the reduced size, the complete absence of user intervention, once the applications have been deployed into the body, and the possibility of these applications to be hermetically sealed. All of these requirements come from the fact that the applications are to be deployed inside the human organism.

An increased challenge exists, when using the human-originated energy sources, because of the limited power densities that these provide. When compared to sources originated in an industrial or outdoor environment, a single human body provides a reduced amount of power.

With respect to the mechanical generation, the movements of the body occur at a very low frequency, and concerning the thermal gradients, the difference of temperature between the human body and the outside environment is not very high, except perhaps, in extreme cold conditions. Moreover, if the body is immobile, a great deal of potentially available mechanical energy is not available. The best place to put a sensor powered by mechanical means would be in a limb, because this zone is prone to have a greater mechanical activity.

The limit values of the power generated from a linearly excited motion-driven generator with linear proof-mass motion, mounted on a walking person, when using a conventional MEMS-compatible and inertial micro-generator strapped to the human body are presented in [40]. These values are between 1 and 4 μW for a device occupying around 0.25 mm^3, rising to between 0.5 and 1.5 mW for a generator occupying 8 cm^3.

In addition, the upper limit of the power generated from a vibration-driven device in a human worn application is presented, which is

$$P_{\max} = 2\frac{Z_l Y_0 \omega^3 m}{\pi}. \tag{2.6}$$

In (2.6), Z_l is the amplitude of the inertial mass motion, Y_0 is the amplitude of the driving motion, m is the value of the proof mass, and ω is the angular frequency of the driving motion. Also in [40], it is assumed that when a person is running at 12 km/h, Y_0 is 0.25 m and the excitation frequency is around 2 Hz.

The light energy source has some drawbacks when used in the human context. These drawbacks are the inexistence of light availability for devices implanted beneath the skin, or the shortage of light for devices worn under clothing. Although light is a very important source of power, it has been shown that thermoelectric devices, also a reliable solid-state technology, are superior to PV cells in the WBAN domain.

For human implantable devices, the thermoelectric generators are receiving increased attention. In order to maximize the amount of power that can be harvested, it is important to match the output impedance of the harvester with the load being supplied, both at the electrical and at the thermal domain. According to [40], the maximum of electric power that can be extracted from a thermoelectric generator is

$$P_{\max} = \frac{(n\,S\,\Delta T_{\mathrm{TEG}})^2}{4R_{\mathrm{T}}}. \tag{2.7}$$

In this expression, n is the number of P and N elements like those in Fig. 2.6, S is the Seebeck coefficient, ΔT_{TEG} is the thermal difference, and R_{T} is the electric resistance of the model of the thermoelectric generator, like the one in Fig. 2.5.

The human body has an almost constant temperature. This temperature is due to the metabolism, which has a power 58.15 W/m^2 over the body surface. A normal adult, with an average surface area of 1.7 m^2, in thermal comfort and regular metabolism, has a heat loss of approximately 100 W. However, the metabolism can provide a value as low as 46 W/m^2, while sleeping, or as high as 550 W/m^2, when running at 15 km/h. During a common workday, sitting at an office, this value can be 70 W/m^2, corresponding to a power dissipation of 119 W and a burn of about 10.3 MJ during a day [41]. The thermal gradient is established between the body temperature and air around the body. Even if the generated energy is not enough to supply a sensor node on a permanent basis, the usual strategy is to accumulate the harvested energy, so that a transmission is enabled from time to time, powering the transmitter with the energy that has been harvested and stored, in the mean time.

In general, as documented in [40], one has power densities of about 300 and 20 μW/cm^3, representing the limits for kinetic and thermal devices, respectively, while the user is running. The values of 30 and 10 μW/cm^3 are the power density limits if the user is walking. The present challenge, which is still under active research, is the means to obtain the correct adaptability for the harvester, in order to match the electric and the thermal impedances, if the body of the user is undergoing a running or a walking regime.

Some specific applications have also been documented, like in [42], where an electromagnetic generator is used both as a harvester and as a sensor, in a situation where the respiratory effort mechanical motion is the energy source. The harvested energy has been shown to be enough to continuously power a low-power microcontroller working with a low data rate wireless link, while monitoring the respiratory rate, and depth, of the user, with good accuracy.

A heel impact absorber harvester has also been developed, to store energy by using human locomotion [17], but in [38], a different approach is taken. Instead of heel impact, the human horizontal foot motion is used. This system uses this energy to charge a rechargeable battery. An interesting feature about this application is the introduction of a MPPT perturb and observe algorithm (which will be addressed in Sect. 4.5.3), optimized for low-frequency human horizontal foot motion, in order to extract as much power as possible. The information provided by the MPPT controller is delivered to a PI controller, in order to establish the optimal switching rate of both a boost and a buck converter. The power density that can be achieved with this application is 8.5 mW/cm^3.

Another way of harvesting energy from human motion has been used in the Sustainable Dance Club [43], where the energy released by dancing people is used to power the light effects in the dance floor zone. The harvesting is performed by using dance floor modules, in the form of tiles. A dancing person can, in average, generate a power of about 2–8 W. In order not to be intrusive to the dancer and to his/her dancing experience, the floor tile is only allowed to displace vertically by a few millimeters, thanks to using a high-stiffness spring. Because of the nature of the involved movement, the working frequency is in the range of 1–2.5 Hz. To match the harvester as best as possible with the load, it is considered that the combination of a single user plus platform weights about 70–100 kg. An additional advantage in this system is the fact that the energy is being locally generated, avoiding the losses

occurred when energy is being transported over the power grid. The measured efficiency for this system was 48 %, including the losses due to the diode rectifier.

The concern about obtaining the intended energy without interfering with the user, so that the harvesting process can be as seamless and unconscious as possible, is also present in [44], where a framework to harvest vibration energy from the human gait is presented. This framework is for calculating the optimal power output for both piezoelectric and electromagnetic vibration harvesters, covering energy harvesting for both walking and running gait of a wide variety of healthy subjects ranging from recreational to elite athletes. The generator is mounted on the lower leg because this is a zone that, because of the foot strike, shows a great acceleration and, simultaneously, allows for conveniently wearing the harvester.

On the other hand, instead of using the sensor in the lower leg, in [45], a miniaturized electromechanical generator, integrated into a human knee prosthesis, is used to power a sensor system inside the prosthesis, enabling it to transmit information about the load on the surfaces of the articulation.

The development of new piezoelectric materials is an active research field. In [46], the fabrication of piezoelectric rubber films and their applications in heartbeat sensing and human energy harvesting is shown. It was demonstrated that the use of the piezoelectric rubber films can function as both sensing and powering elements and potentially realize the integration of human physiological monitoring and energy harvesting.

The human body can even be used to harvest energy from electromagnetic radiations. According to a study performed in [47], it has been shown that the properties of the human tissues, which have a high dielectric constant, especially at low frequencies, are much suitable to receive the electromagnetic radiations of low frequency, emitted by the power lines in an indoor environment. Moreover, using an antenna would be very difficult to capture the same radiation because of the low frequency band and the narrow bandwidth. The harvested energy can be delivered to an application by simply making contact with the human body.

In [47], measurements were made in order to determine the effective length of the human body. The effective lengths had maximum values (about 5 cm) at about 40 MHz, which is large, considering the poor conductivity of body tissues. With higher and lower frequencies, the length decreases. In addition, measurements also included the estimated voltages received by the human body, which varies from place to place, according to the frequency predominance in the environment.

Another work that also studies the theme of electromagnetic energy harvesting using the human body can be found in [48].

2.1.5 Microbial Fuel Cells

The microbial fuel cell (MFC) principle is based on the electrochemical reactions that bacteria produce when in activity. The energy generated by these reactions can be harvested, similarly as with the other sources already addressed.

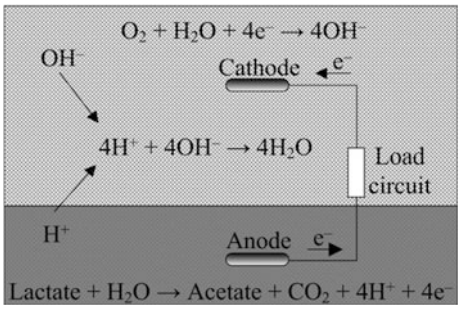

Fig. 2.9 MFC structure and electrochemical reactions

At environments where it is very difficult to reach, in electronic applications that have been deployed, like in underwater monitoring systems, there have been successfully tried several ways to power such applications by using the bacteria that live in the water. In [49], the MFC consists of two electrodes (one anode and one cathode), in which the anode is buried in the seafloor and the cathode is left suspended in the water. On the anode side, there is a type of bacteria, the *Shewanella oneidensis*, which breaks down the lactate in the water and makes it to release electrons and react with water. The basic structure of the setup and the chemical reactions that occur are schematically shown in Fig. 2.9, and the reaction just mentioned appears at the bottom of it.

The electrons produced in the seafloor ($4e^-$) travel to the anode and then to the cathode, through the load of the MFC. On the other hand, the protons produced by this reaction ($4H^+$) travel to the cathode side, through the water.

On the cathode side, the electrons from the anode react with water and with the oxygen in the water, to produce $4OH^-$, as shown by the chemical equation at the top of Fig. 2.9. Ultimately, the reaction of OH^- produced at the cathode, with H^+, coming from the anode, ends up forming water ($4H_2O$). Neither of the electrodes gets corroded, because the chemical reactions just described do not include any other material than those that were mentioned. Moreover, the net product of the chemical reaction is not some polluting compound. One topic that must be carefully addressed is the surface area of the electrodes, because this factor has a key role in the power density that can be achieved.

Generally, the voltage and the current that can be generated are weak, requiring an adequate power management system to interface the MFC with the load and having to encompass a storage device. Thus, the load can only work intermittently, in order to correctly meet the demand of power and for short periods of time. However, an application like the one described is self-contained, renewable, maintenance-free, and operational (on an intermittent basis), in a water environment.

Another environment, where there is an abundant quantity of bacteria, is in wastewater. This environment is very hostile to humans, so the use of a WSN that requires no human interventions after deployment is unarguably preferable. Another place, with similar problems, is the water tanks of nuclear plants. As such, under the subject of monitoring and control of wastewater treatment plants

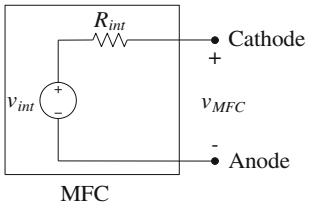

Fig. 2.10 Electrical model for a MFC

(WWTP), in [50] it is suggested a system that seeks to have an efficient use of electrical energy in these facilities, as the standards for processed water tend to be increasingly tightened. The architecture of the nodes of a WSN for this purpose makes use of field programmable analog arrays (FPAAs) and low-power networking protocols, and the powering of the nodes is done by using MFC that harvests energy from the wastewater to which it was deployed. The harvested energy, as usual, is very scarce and so the use of FPAAs represents a much reduced power dissipation, when compared to their digital counterparts, the field programmable gate arrays (FPGAs), and the advantage of having a kind of parallel computing, since there is no central processor.

The electrical model of a MFC is shown in [51]. This model is represented in Fig. 2.10.

As it can be seen, the model is a Thévenin equivalent, similar to the model established for the thermal gradient energy source, shown in Fig. 2.5. The internal resistance of the MFC (R_{int}) is the sum of the system ohmic resistance, charge transfer resistance, and activation resistance. The internal voltage and resistance can vary nonlinearly, as the MFC condition changes. Possible causes for such changes include instantaneous output power level, accumulated extracted energy, bacteria community and activity shifts, and environmental condition changes. The thermodynamic limitations determine that v_{int} will have a maximum value of 0.8 V and a current output in the range of a few mA. In order to extract the maximum power out of the MFC, a load with the same value as R_{int} must be used, meaning that v_{MFC} will drop to half of the value of v_{int}. According to the intended application, this value may not be sufficient, and special measures must be adopted. With the MFC characterized in [51], the values obtained were $v_{\text{int}} \approx 0.65$ V and $R_{\text{int}} \approx 86\ \Omega$. Thus, when extracting the maximum power, the output voltage will be around 0.33 V.

The work performed in [52] suggests a new type of construction for MFCs, which is called single-chamber microbial fuel cell (SCMFC). This type of MFC uses stainless steel attached to the anode and the cathode which showed to help in the constancy of the developed voltage over time. In addition, the pH of the solution inside the MFC became lower (acid). This fact caused the stainless steel plates that were used to help in the process to suffer some corrosion.

There is another system documented in the literature [7], using a multi-harvest platform, and among the sources that are used, there is a MFC.

2.1.6 Light

In particular, light is an electromagnetic wave, with the particularity of being visible. There is an interval of frequencies that comprises the visible light. In the lower end of this interval, light tends to be red, and as the frequency moves to higher values, light goes through the known colors, and in the upper end, it gets violet. Thus, light is bounded by infrared and ultraviolet. In Fig. 2.11, the entire electromagnetic spectrum is shown, with emphasis in the visible range.

In this spectrum interval, since the frequency values are already very high, it is more common to use the wavelength, instead of the frequency value, to identify the spectrum zone under consideration.

The spectrum outside the atmosphere, also known as the 5,800 K blackbody, has the designation of AM0 (Air Mass 0), meaning "zero atmospheres." This is the standard used to characterize PV cells to be used in space, for example, to power satellites.

The sunlight, after penetrating the atmosphere, at sea level, perpendicularly to the surface of the Earth, has a spectrum which is referred to as AM1, meaning "one atmosphere." AM1 is useful for estimating the performance of PV cells in equatorial and tropical regions. The index "1" is related to the angle of solar incidence, which is minimal in this situation.

However, in Europe and in similar latitudes of the North and South hemispheres (where there is a great deal of population and industrial centers), the incidence of the Sun over the surface of the Earth has a different angle than in the equator. This angle is about 42° from the horizontal line, so sunlight must cross a greater amount

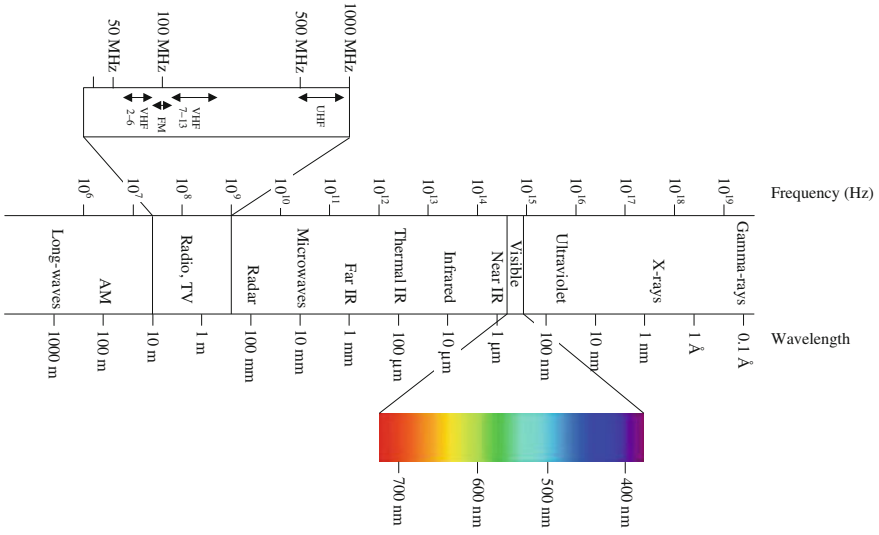

Fig. 2.11 The electromagnetic spectrum

of atmosphere. As such, the spectrum is referred to as AM1.5, which means "one and a half atmospheres," on a clear day. This value is the standard test situation for terrestrial PV panels. However, for higher latitudes, there are more air mass indexes, used for higher incidence angles, above 60°. These indexes can go until AM38, in the polar zones, where the incident angle is close to 90°.

In any of the above cases, atmospheric pollution, clouds, or fog also have an influence on the amount of irradiated energy that can reach the surface of the Earth, due to the obstruction that they present.

According to AM1.5, after crossing the atmosphere, and at the maximum of its intensity, the light from the Sun can provide about 1 kW/m^2 across the whole wavelength spectrum. The irradiated light energy that the Sun produces is different according to each wavelength. To have an idea of this, the power spectral density of the solar radiation is shown in [53]—Plate 1, where the top curve represents the solar spectrum just outside the atmosphere. The total power density in this zone is 1.366 kW/m^2, which is known as the solar constant. The curve filled with yellow is the standardized solar spectrum on the surface of Earth, for performance evaluation of PV cells (AM1.5), and the standard power density under these conditions is about 1 kW/m^2, as it has already been referred. The dashed curve is the solar radiation spectrum at the position of Earth by modeling the Sun as a blackbody radiator at 5,800 K. As shown, the solar spectrum just outside the atmosphere, the AM0 spectrum, matches well with the blackbody radiation spectrum at 5,800 K, diluted by the distance from the Sun to Earth. The relation with human vision of the color spectrum is shown in the bar beneath. As shown in the referred figure, only about one half of the solar radiation power is in the visible range [53].

Next, in Fig. 2.12, the average annual amount of insulation hours for the European continent and some countries of the Middle East and the North of Africa is shown.

From this map, it can be seen that Portugal, Italy, Greece, and Spain have the highest potential for solar photovoltaic electricity generation in the European continent, as opposed to the countries of the north, in which the amount of solar radiation is undoubtedly smaller.

The solar energy is the primary source of energy to the planet, and it reaches it in an enormous amount. This is why light has the largest energy density, when compared to the other harvestable sources. According to [53], if one takes into account the total power of solar radiation reaching Earth, it will be about 1.73×10^{17} W, meaning that the total energy of solar radiation reaching Earth, each year, is 5.46×10^{24} J = 5,460,000 EJ. In the period of 2005–2010, the average energy demand in the planet, every year, was about 500 EJ, which means that less than 0.01 % of the total solar energy reaching the planet would be enough to satisfy all the energetic needs of the world. However, not all solar radiation that irradiates the atmosphere reaches the ground, because about 30 % of solar radiation is reflected into space. In addition, about 20 % of solar radiation is absorbed by clouds and molecules in the air and also about 75 % of the surface of Earth is water. Thus, even if only 10 % of total solar radiation was utilizable, only 0.1 % of it could power the entire world [53].

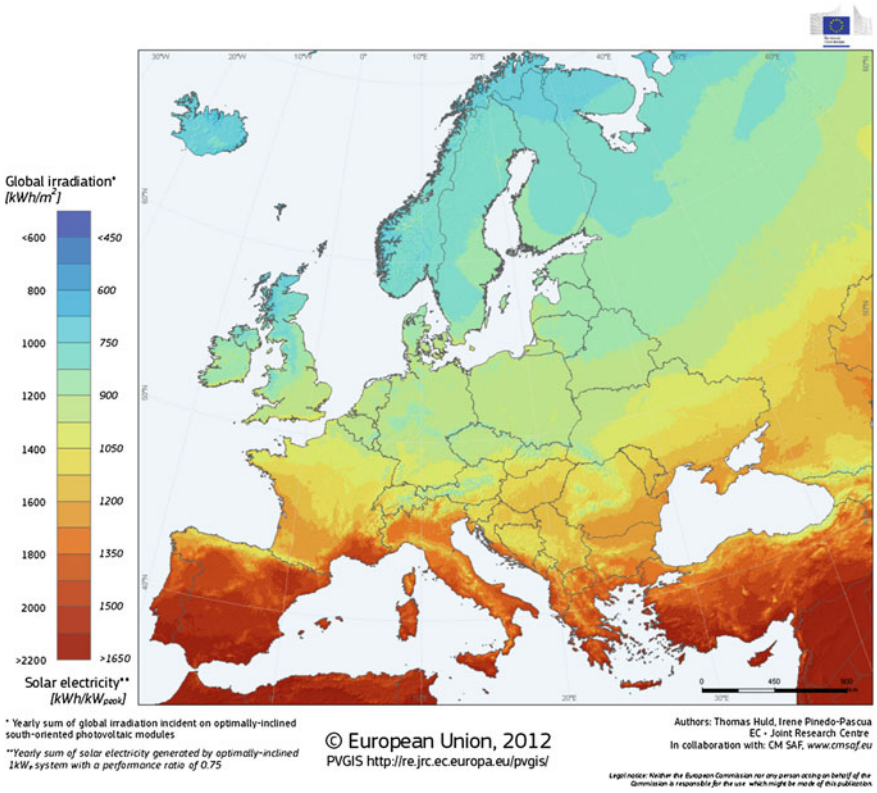

Fig. 2.12 Photovoltaic solar electricity potential of Europe and some zones of the Middle East and the North of Africa (PVGIS © European Union 2001–2012) [54, 55]

In indoor energy harvesting applications, the amount of light energy that is available is, however, much more reduced. The available light energy in indoors can vary significantly, since the light from the Sun is attenuated and can be mixed with artificial light. The literature reports available indoor irradiances ranging from one tenth of the maximum Sun intensity [18] to about 0.833 W/m^2 (100 lux converted to W/m^2 using [56]) in a lightly dimmed room [57], or 10 W/m^2, when the PV cells are placed very close to lamps [58].

The conversion principle indicated in [56] takes into account the nature of the wavelength spectrum in indoor environments. In this kind of environment, there is a predominance of artificial light, provided by light bulbs or light tubes. The latter have such a spectrum, leading to the application of the conversion factor to be

$$E_{\mathrm{rad}}(\mathrm{W/m^2}) = \frac{E_{\mathrm{rad}}(\mathrm{lux})}{120}. \tag{2.8}$$

Given the unit of light intensity, the lux (lx), according to some authors, there is a correspondence between the amount of power by unit of area and the amount of incident light, and it is defined under the relation that 1 kW/m^2 = 683 klx, i.e., 1 lx = 1/683 W/m^2, used in [59, 60], for example. This conversion does not take into account the fact that the light has a specific indoor spectral pattern. According to [59], the level of indoor lighting is still enough to power electronic applications, namely from overhead fluorescent lights, with 34 W of power.

In [61], it is documented how the amount of available light energy is typically distributed along the day, accounting for the effects of fixed artificial irradiance and variable natural irradiance. It is shown that, in an indoor environment, the most optimistic value is about 5 W/m^2 (600 lux), achieved at about 13 h 30 min. Most of this illuminance is provided by artificial lights, and any energy harvesting function can only be useful in the period from 04 h 00 min to 21 h 00 min.

In some situations, it proves useful to have a history of the typical solar irradiation of the location where the harvester system is to be placed [62, 63]. In [64], a study is made and it is shown that using weather forecasts for predictions in both solar- and wind-powered sensor systems increases each system's ability to satisfy its demands compared with existing strategies. Depending where the system is to be located, the variability of the light source can depend over time. Only in indoor environments, one can consider that there is any constancy, but this condition is not always true.

The key element for light energy harvesting is the PV cell. This solid-state device converts light energy directly to electrical energy without using any moving parts. A PV cell is basically a photodiode, and it can be manufactured in CMOS technology [65, 66].

When the PV cell is illuminated, its output behaves like a current source in parallel with a diode, the latter acting as a voltage limiter. PV cells are characterized by three main parameters: the maximum power point (MPP), the open-circuit voltage (V_{OC}), and the short-circuit current (I_{SC}). The PV cell can be modeled by an equivalent electric circuit shown in Fig. 2.13a, characterized by the parameters of the equivalent circuit (I_1, R_P, and R_S). The parameters of the diode device (D) also play an important role according to the amount of illumination that the PV cell is subjected to. In Fig. 2.13b, a typical plot of the power and the current produced by a PV cell is shown, letting know how these functions look like, as a function of the output voltage v_{out}. The power function of the PV cell is obtained by multiplying the output voltage, v_{out}, by the output current, i_{out}. The MPP of the power function is achieved with an output voltage which is about 71–78 % of the open-circuit voltage of the PV cell [67], varying as the light or the temperature varies. The tracking of the true MPP is an active area of research, corresponding to the MPPT problem, which will be addressed in Chap. 4—Sect. 4.5.

The output current of the PV cell (i_{out}) is related to the remaining elements of the model, according to the following equation:

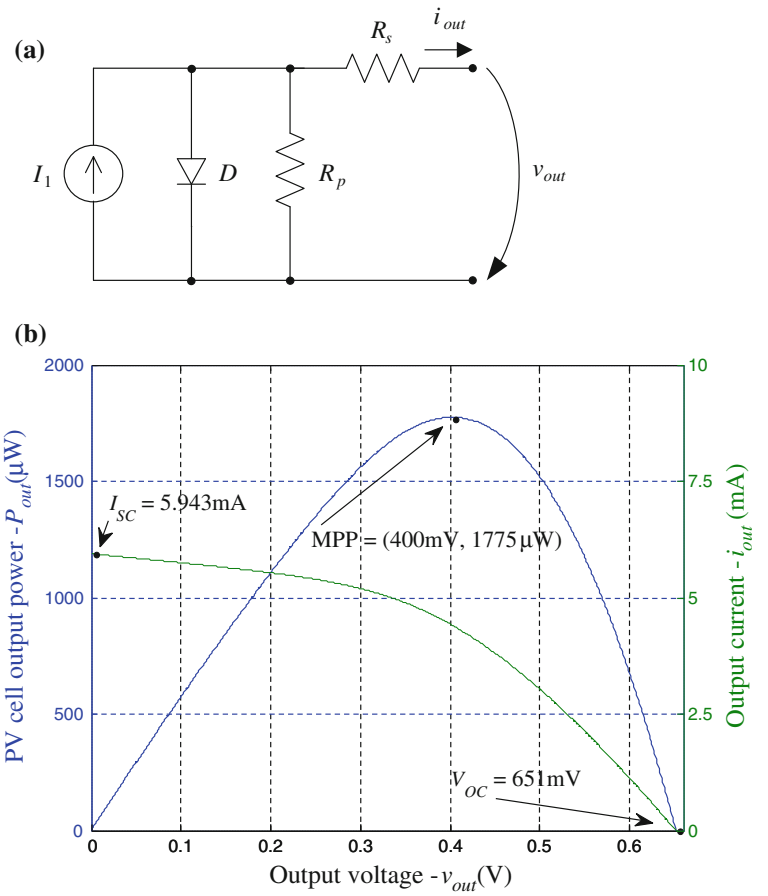

Fig. 2.13 **a** Equivalent electrical circuit of a PV cell, **b** example of typical current and power curves, as a function of the output voltage

$$i_{\text{out}} = I_1 - I_S\left(e^{q\frac{v_{\text{out}}+R_s i_{\text{out}}}{nkT}} - 1\right) - \frac{v_{\text{out}} + R_s i_{\text{out}}}{R_p}. \tag{2.9}$$

In this equation, I_S is the limit of the current in the diode under high reverse bias. If the diode did not exhibit breakdown, the maximum reverse current that one could get through the diode, with an infinite reverse bias, would be I_S. Another definition for it is that it is the "dark saturation current," i.e., the diode leakage current density in the absence of light. Also, q is the electron elementary charge ($1.60217657 \times 10^{-19}$ C) and k is the Boltzmann constant ($1.380648813 \times 10^{-23}$ J/K). T is the ambient temperature, expressed in K. The factor n is the emission (or ideality) coefficient, which equals 1 for an ideal diode.

Although it is possible to build a PV cell using CMOS technology, it is not simple to integrate PV cells with other circuits in the same die, in order to obtain a complete system on chip (SoC) [68, 69]. The PV cell causes a positive voltage in the substrate, thus causing a possible latch-up condition in the die. Also, when a series connection of several devices is required, the fact that the diodes are built on the same substrate may be limiting [70]. This limitation has become evident in a PV cell that was manufactured and that appears reported in Chap. 3—Sect. 3.5. To cope with these limitations, it is necessary to use more expensive technologies, such as silicon on insulator (SOI), which allow for building an almost indefinite number of series connected to PV cells, if one wants to obtain a higher voltage value [71].

The efficiency of the most common PV cells is still relatively low, at about 20 % [18]. In indoor environments, amorphous silicon PV cells can have efficiencies up to about 7 % [59]. However, there are some PV cells that can reach efficiencies as high as about 50 %, as claimed in [72], although involving the use of new layout architectures and less common materials, resulting in more expensive systems.

In order to try reducing the production costs, it is possible to use PV cell technologies with lower efficiencies, but that also have lower manufacturing costs, resulting, however, in a larger area for the PV cell, for the same level of output power. Using amorphous silicon PV cells is an example of such a trade-off, in which costs are lower, but at the expense of a larger area to obtain the same level of power [73]. In [61], the differences of the power densities measured on crystalline silicon and amorphous silicon solar panels are illustrated, when different light sources are used to generate the same illuminance level. It is shown that in indoor environments, as opposed to crystalline silicon PV cells, amorphous silicon PV cells do not suffer a strong reduction in their power density, when the source of light changes from sunlight to fluorescent lights. Thus, this evidence is indicating that the amorphous silicon-based PV cells are more suitable for indoor applications.

Nonetheless, if the overall cost is one of the most meaningful factors, this option will also have to be taken into consideration to preserve commercial competitiveness.

There are some other devices that also deal with the harvesting of light energy. These devices are the photosynthetic electrochemical cells (PEC). This kind of cell can generate power both under light and dark conditions, and the principle of the operation of such a device is based on photosynthesis, similarly to plants. This principle is based on a biosolar process, such that one has production of electrons with light (photosynthesis): $CO_2 + H_2O \rightarrow (CH_2O) + O_2 + e^-$ and with dark (respiration): $(CH_2O) + O_2 \rightarrow CO_2 + H_2O + e^-$ [74]. Photosynthesis and respiration processes are both involved with an electron transfer chain. Similar to the construction of the electrochemical cell, the PEC is made up of an anode and a cathode, separated by a proton exchange membrane (PEM).

The photosynthetic microorganisms form the anode portion, and there is an electron acceptor on the cathode side. A gold electrode is fabricated for the device on top of a proton exchange membrane, which accepts only the positive ions and blocks the electrons. The free electron that is produced is trapped by the electrode. An electric circuit connected to the electrode forms a path, and the electron is made to flow through, thereby producing electrical energy. Preparing an external circuit

and integrating it with the photosynthetic process enables the flow of electrons in the desired direction, resulting in current.

PECs can be considered to belong to the category of the microbial fuel cells, which were described in Sect. 2.1.5.

2.2 Comparison of Harvestable Energy Sources

It has been seen that there is a reasonable number of ambient sources that can be harvested. The source that will be harvested is dictated according to the intended application and the energy availability. However, as seen before, a system may even not limit itself to a single source, but for the sake of simplicity, a single source is preferable. Placing all sources side by side, the one that shows the highest power density by volume unity is the light energy, followed by mechanical and thermal energy, respectively [1]. It is also important to point out that the operation of converting light energy to electrical energy (using a PV cell) is one of the easiest and cheapest energy conversion operations. Therefore, in most cases, powering the sensor using light energy is always the best option. The only exception is when the sensor is located in a human (or animal) body. In this case, it would be convenient to use thermal or mechanical energy, for example.

Table 2.1, presents some demonstrated capabilities of energy sources and their respective energy densities. This table is adapted from [17], to which some more

Table 2.1 Demonstrated capability of some energy sources, regarding their density and performance, and examples of scenarios where to scavenge such energy sources

Energy source	Energy density/performance	Short examples of scavenged environments
Ambient radio frequency	<1 $\mu W/cm^2$	Anywhere, mainly in urban areas
Ambient light	100 mW/cm^2 (directed toward the bright Sun) 100 $\mu W/cm^2$ (illuminated office)	Anywhere, where natural or artificial light is available
Thermoelectric	60 $\mu W/cm^2$	Furnaces, exhaust pipes, combustion engines, human warmth
Vibrational micro-generators	4 $\mu W/cm^3$ (human motion—Hz) 800 $\mu W/cm^3$ (machines—kHz)	Machines with rotating engines, human movements
Ambient airflow	1 mW/cm^2	Anywhere, where air shows a consistent and abundant flow
Push buttons	50 μJ/N	Human action over buttons of commands
Hand generators	30 W/kg	Human action over specific mechanical generators
Heel strike	7 W potentially available (1 cm deflection at 70 kg per 1 Hz walk)	Using shoe insertion, by human walking motion

information has been added, about contexts where the energy can be harvested. The data presented in this table serve to have an idea of how much energy is to be expected from a given source and also to have a comparison among the various sources.

2.3 Energy Harvesting-Based Sensor Networks

2.3.1 Introduction

Wireless sensor networks, whose nodes make use of harvested energy, have interested researchers not only in the adaptation of the nodes to the environments in which those networks can be deployed in, but also in the development of methods and optimization of parameters to extend the operation of the nodes.

Perhaps, the most critical factor concerning these networks is the energy availability, because if that cannot be guaranteed, the whole network can be compromised. However, there are also some other parameters that must be taken into account, in addition to the energy availability. These parameters are the operational lifetime of the node, the sensing reliability, the transmission coverage that the node can provide, and also the cost of the investment, which should be as much affordable as possible.

Typically, the harvesting module inside each node in a sensor network provides some sort of energy storage in order to hold enough energy to power the node during any period in which there is not available energy to be harvested. This kind of storage is normally done by using a device such as a battery or a supercapacitor. The storage device is charged when there is energy being harvested, and discharged, by making use of the stored energy to power the node, in case of need. If the node is provided with processing capabilities, such that it can predict when will begin its next charge cycle, it can execute the convenient or allowable set of operations that optimize the working time, extending it as much as possible, so as to have an effective utility, while consuming energy as moderately as possible. This rationalization can be done by reducing the sampling rate, the transmitted power, or the duty cycle of operations [75].

2.3.2 Energy Neutrality

With regard to the management of the energy that is harvested by a node, if this energy is more than the energy being consumed, over a period of time that can be supported by the energy buffers, then the node can operate with a continuous lifetime. This kind of situation is known in the literature as the Energy Neutral Operation (ENO) [76]. However, the excess of energy is wasted, instead of being used for increasing the performance of the system. Thus, it can be considered that

the node is not operating in a fully efficient fashion. The desired operating regime is when the harvested energy is approximately the same as the consumed energy, while all the harvested energy is put at the service of the performance of the system. Operating in such a way is named in the literature as ENO-Max [77]. This type of operation constitutes one of the most important goals of WSNs being powered by energy harvested from the environment, because the system will be conveniently sized to strictly meet the requirements of operation, avoiding waste of resources and increase of costs, due to an eventual system oversizing.

2.3.3 Examples of WSN Powered by Harvested Energy

The deployment of WSN can be done to a variety of scenarios. As it could already been seen, almost ever, the use of a given type of energy source is determined according to the type of environment in which the network resides. Next, some examples will be given of such networks.

2.3.3.1 Health Condition Monitoring

The work reported in [41] concerns about a WBAN in which a number of nodes take place. This network has the purpose of monitoring various vital signs and to collect healthcare data for medical diagnosis purposes, by using different types of physiological sensors onboard of the sensor nodes. These include devices such as the electrocardiogram (ECG) sensor, electromyography (EMG) sensor, electroencephalography (EEG) sensor, blood pressure sensor, tilt sensor, breathing sensor, movement sensor, and thermometer. The objective is to gather patient information in a database, in order to have enough data to make a good diagnosis when that becomes urgent by medical staff. There is an additional feature to the nodes, which is the detection of the fall of the patient, by using an accelerometer.

The nodes in this WBAN are supplied by thermal energy, harvested from the body warmth of the patient. An interesting feature about this network is the fact that the nodes can rotate their role about the gateway function. Instead of being just one of the nodes dedicated to that purpose, each node was given the capability to be a gateway. As this is a much power consuming function, and since transmission is not performed during all the time, different nodes, at each time, serve as a radio interface between the WBAN and the backbone of the healthcare network.

2.3.3.2 Forest Surveillance and Monitoring

Another scenario in which a WSN proves useful is in forest monitoring, for prevention of forest fires. Under this purpose, [78] presents a network whose nodes have their computational capability based on a microcontroller. Each node is

equipped with a smoke sensor and an infrared flame detector. Ideally, such a network is intended to replace the traditional forest surveillance, such as ground patrolling, watchtower detecting, aerial patrolling, and space satellite detection. Any of these methods is expensive and involves a great deal of human intervention. The deployment of such a network occurs with each node randomly put to the field, and self-organizing together with the other nodes, in order to form a distributed network by protocol. Then, the gathered data can start to flow among nodes, by using the wireless communication interface, and finally, it can be transmitted to the monitoring center. Then, the data can be processed and analyzed by the monitoring host computer, to provide visual information for forestry experts or for whichever decisions that should be taken or alarms that should be activated. Each node is put to work by using a low duty cycle and uses solar energy harvested by a PV cell in order to charge a rechargeable battery.

2.3.3.3 Energy and Environment Monitoring in Buildings

Another area under strong interest from researchers and the general public is domotics and intelligent buildings, namely Building Energy and Environment Monitoring (BEEM). This kind of monitoring has the objective to use energy more rationally, allowing for an overall reduction of energy consumption and carbon emission, while reducing the present costs associated with this kind of monitoring. Several works have been published in this field, and among which, [79] is an example. In this work, a WSN with sixty two nodes is deployed to an office building. Each node contains a microcontroller, for computational purposes, and carries multiple sensors, making it capable of measuring energy consumption, light level, temperature, and humidity parameters. Also, each node is able to transmit data using a 2.4 GHz *Zigbee* (IEEE 802.15.4) interface.

In this work, it is claimed to have designed the world's first known indoor light energy harvesting powered BEEM system. The nodes are powered by light energy, harvested in an indoor office environment, using a PV panel with 85 mm × 50 mm. The harvested energy is stored in a supercapacitor, so that the node can continue to operate during the periods when no light is available. This application has succeeded in monitoring the desired parameters continuously for an entire month, requiring no user intervention.

2.3.3.4 WSNs in Automotive Applications

In an automobile vehicle, the need to keep the quiescent current of the battery as low as possible, in order to extend its durability, has led to the development of applications that use harvested energy as the power source. As such, in [80], an intrusion detection system is powered by harvested energy. This system consists of a wireless network of sensors, whose function is to detect the breaking of glasses caused by burglar assault.

In this application, special care has been taken, regarding the communication among the nodes, which include built-in safety features such as plausibility checks, encryption, and radio channel monitoring, with special focus being laid on the medium access control (MAC) layer protocol design.

The development of automotive applications has an inherent set of demands that must be addressed. For example, the electronic circuits must be prepared to withstand extreme temperature conditions, as well as humidity. In addition, as the automobile market is global, the regulations about wireless networks and alarm systems must always take the international regulations into account. Another requirement specified by the automotive industry is that with full functionality, a period of more than six weeks can be bridged without recharging the storage device of the sensor node, which can be a rechargeable battery or a supercapacitor. Also, the system has to be connected to the controller area network (CAN) bus of the vehicle.

With the vehicle regularly in use, there are various energy sources that can be harvested: Light is accessible through the ceiling and glasses; heat can be harnessed from the exhaust system; or vibrations from the engine or the moving structure are also available. However, when the car is parked for a long period of time in a dark garage, none of these sources is available. As a consequence, the WSN that implements the intrusion detection system could be disabled. To counter for this eventuality, the nodes are kept sleeping for most of the time and, when in activity, the MAC protocol that is used is much energy efficient.

The limited spatial environment in which the network resides avoids the need for a routing algorithm, as well as it allows for a small payload to be transported in the messages, keeping the protocol as short as possible. In [80], the network is composed by seven nodes plus a base station, in which the latter is connected to the CAN bus, so that the messages can be processed by an electronic module in the car. Moreover, it must be taken into account that, if the car is parked in a parking lot, there is the possibility to exist cross talk due to networks installed in nearby cars. The protocol that is used accepts longer transmission times, due to a very long preamble. It is possible to let the receivers to stay idle or sleeping for most of the time. A receiver wakes up periodically for just a small interval, to listen to the channel. If the channel is idle, the receiver returns to an energy-saving mode.

The sensor nodes are powered by a mechanical energy harvester, and since the glass break sensor is purely passive, it must be polled by a microcontroller, which sleeps in between samples. Only in case of glass break detection, the sensor node immediately tries to contact the base station to report the glass breakage with multiple alarm messages, until the sensor node receives an acknowledgment message from the base station, or the energy storage device is empty. This activity profile allows the WSN to hold for about six weeks without recharging the storage device, while keeping all safety features required by the automotive industry.

2.3.3.5 Structural Health Monitoring (SHM)

Structural health monitoring (SHM) is useful in many contexts. This is the process of detecting damage in aerospace, civil, and mechanical infrastructures [81]. The sensors can be deployed to any structure that needs monitoring, such as vehicles, buildings, bridges, and monuments.

The detection method can consist of an operation of statistical pattern recognition, requiring four sequential steps: operational evaluation, data acquisition, feature extraction, and statistical modeling for feature classification. The goal of any SHM sensor network is to make the sensor reading as directly correlated with, and as sensitive to, damage as possible, so that the network can adequately observe changes in the system dynamics caused by damage and manage these data for suitable signal processing, feature extraction, and classification. Thus, it is very important to make the sensors as independent as possible from all other sources of environmental and operational variability, and independent from each other, while providing maximal data with the minimum number of sensors. Toward these requirements, there are a number of specifications that must be previously established, such as types of data to be acquired; sensor types, number and locations; bandwidth, sensitivity and dynamic range; data acquisition/telemetry/storage system; power requirements; sampling intervals; processor/memory requirements; and excitation source needs (for active sensing).

Regarding how the hardware is chosen, five issues must be addressed: (1) the length scales on which damage is to be detected, (2) the timescale on which damage evolves, (3) the effect of varying and/or adverse operational and environmental conditions on the sensing system, (4) power availability, and (5) cost.

The most common measurements made for SHM purposes are acceleration and strain. Acceleration is the most used measurement in SHM, because of the maturity of the technology associated with accelerometers, as well as of the hardware that performs the signal conditioning. However, these devices are mostly used in wired networks, where the voltage of the sensor is transferred to a data acquisition central unit, where it is processed. This kind of procedure is much power consuming, especially because of the number of sensors that may be involved, so accelerometers in MEMS technology can start to be used more often, so as to counter this problem. After acceleration, strain is the most measured physical parameter in SHM. The technology of strain gauges in also mature and the signal is typically measured using a bridge circuit, and also including the signal conditioning, they consume power at a much commensurate level. The most common strain gauge technology is the electric resistive foil gauge, but there has been an increase in the use of fiber optic solutions to strain measurement, although the power requirements are higher than with strain gauges. The two dominant fiber optic technologies are direct fiber interferometry and fiber Bragg gratings (FBGs). Most commercial systems today take advantage of FBG technology.

Today, two sensor network paradigms exist for SHM, which are having the sensor arrays directly connected to the central processing hardware and the wireless decentralized sensing and processing. Each has advantages and disadvantages.

The first has the advantage of being widely commercially available, both in devices and in complete systems. However, it has the disadvantage of being wired and requiring AC connections due to the power consumption that it represents.

The wireless decentralized sensing and processing has been under the strong interest of researchers, regarding many aspects already referred in this text, such as power dissipation and communications, overcoming many limitations of the wired networks. Ad hoc networking and hopping are usually adopted, with some problems concerning it, like the fact that the nodes closer to the base station are more subjected to data collisions and, as most of the total traffic passes through them, their power source drains out more rapidly. Researchers are also studying the advantages of having mixed wired and wireless networks, in order to explore the advantages of both.

As with every vehicle, aircrafts are prone to have WSN to monitor parameters related to the SHM of body parts made of carbon or glass fiber reinforced plastic [22]. The use of wireless nodes is helpful, because it avoids wiring, thus reducing costs, installation complexity, and weight. The latter is critical, regarding the fuel consumption.

2.3.3.6 Wireless Networks for Localization or Study of Animals

The subject of animal localization, animal behavior, cattle monitoring, or the improvement of livestock-related techniques has been an active research areas for years. In [82], a WSN mostly kinetically powered has been used for the localization of herds in grazing areas. This network has primary and secondary nodes. Primary nodes are battery powered and serve to collect information transmitted by the secondary nodes, as well as position and time data, to a base station that monitors all the animals. The secondary nodes are attached to the animals and are powered by a mechanical transducer, which generates electrical energy from the motion of the animals. These nodes have the function to broadcast their identification.

The main objective of the work in [82] is to remotely track the movement of animals in herds, such that a herder may know where the herd is, if any animal has left, or where it was lately around. This work was tested with semidomesticated scandinavian reindeer. Instead of using methods such as global positioning system (GPS) tracking, which are expensive and power consuming, in each animal, a kinetic harvester module is used, which powers a transmitter that can reach up a hundred meters. The nodes are batteryless and require almost no human intervention. Only the primary nodes, which are powered by a battery, get their position by GPS. The secondary nodes use a rectifier, as usual with mechanical energy sources, and a supercapacitor to store the harvested energy. A 20-cm magnet/coil generator has been used as the kinetic-to-electric energy converter. The whole circuit powers a radio transmitter. The node is attached to the animal, by using a collar.

The nodes mounted on the animals were able to transmit and be detected more than three times per hour, in average, without the need of any battery, proving that the concept is feasible.

There are other situations, in which the study of wildlife has led to the deployment of electronic applications powered by harvested energy. As an example, two of them will be mentioned here, although these have been referred in [75, 82].

The first one is the *ZebraNet*, which is a network of GPS sensors to track zebra movement and long-term animal migration patterns, habitats, and group sizes. The nodes in this network are also attached to the neck of the animals with a collar and are powered by solar energy, which is much abundant in the habitat of these animals. The collar has 14 solar modules, a comparator and a boost converter that charges a Li-ion rechargeable battery, so that the node can be powered during nighttime and bad weather. The battery allows for 72 h of operation, when completely charged. The peak output power is 400 mW. The node is also composed of a microcontroller which controls the operations of the system, as well as the charging of the battery.

The second one is the *TurtleNet*, whose function is to track turtles. Similar to the *ZebraNet*, the nodes in this network are also powered by a PV cell that outputs 90 mW at 4.2 V. Moreover, these nodes must be waterproof, because turtles spend much of their time under water.

In [75], there is more information about each of these networks, as well as the indication to the original references that explain all the details.

2.4 Conclusions

In this chapter, an overview about energy harvesting systems was made. By performing a search in some of the available literature, information was collected about the ambient sources that can be harvested and systems that make use of those sources to power themselves.

According to the type of source that is being harvested, a convenient harvester device must be used and it is an important tool to have a model able to electrically describe how the harvester works. This functionality is particularly important in the design phase, in order to model and simulate the whole system, also encompassing the harvester.

Moreover, for a particular kind of source, there are already certain types of circuits that are strictly required to be used, like the case of rectifiers in RF and in mechanical energy harvesting, for example.

If the deployed systems are able to operate in a self-powered fashion, this brings out a lot of benefits, cost wise. This operation, installation and maintenance philosophy, greatly reduces the amount of money needed to keep the system at work. For instance, when looking at installation costs, not needing to connect to the power grid means that wiring and additional equipment is not needed. As a consequence, there is no need for manpower to take care of an elaborated system installation. When looking at the maintenance costs, as the infrastructure is wireless, anything related to cables or similar, and related equipment, does not apply. An expression that can serve to illustrate the intended operation paradigm is "*deploy and forget*" [83].

For systems powered by light, one maintenance factor that should be taken into account is concerned with the hypothetical periodical cleaning of the PV cell, as dust can accumulate over time and deteriorate the harvesting characteristic.

Since the amount of available energy, which can be harvested, is typically very low, and the resulting voltages are also low, these systems must use a voltage elevator, in order to provide a suitable voltage to power an electronic application. In addition to this requirement, there is also the need to provide some means to store the harvested energy so that the load system can be supplied even when there is a shortage of energy from the chosen harvested source. These topics will be addressed in Chap. 4.

The overview that was given in this chapter had the purpose of introducing to the energy harvesting theme. This was done by showing, with some examples of published material, what are the available energy sources, the main parameters and computational infrastructures that must be accounted for, some systems that already exist, and the challenges that one must face when designing a system for such a class of applications. As such, the reader is invited to deepen the search that has been made and presented here, in order to match this search with the real demands to be met, as the material presented in this chapter is only introductory.

References

1. Chalasani, S., & Conrad, J. M. (2008). A survey of energy harvesting sources for embedded systems. In *Proceedings of IEEE Southeastcon 2008*, 3–6 April 2008, pp. 442–447.
2. Chou, P. H., & Park, C. (2005). Energy-efficient platform designs for real-world wireless sensing applications. In *Proceedings of the IEEE ACM International Conference on Computer-Aided Design (ICCAD-2005)*, 6–10 November 2005, pp. 913–920.
3. Lhermet, H., Condemine, C., Plissonnier, M., Salot, R., Audebert, P., & Rosset, M. (2008). Efficient power management circuit: thermal energy harvesting to above-IC microbattery energy storage. *IEEE Journal of Solid-State Circuits*, *43*(1), 246–255.
4. Tan, Y. K., & Panda, S. K. (2011). Energy harvesting from hybrid indoor ambient light and thermal energy sources for enhanced performance of wireless sensor nodes. *IEEE Transactions on Industrial Electronics*, *58*(9), September 2011, pp. 4424–4435.
5. Saggini, S., Ongaro, F., Galperti, C., & Mattavelli, P. (2010). Supercapacitor-based hybrid storage systems for energy harvesting in wireless sensor networks. In *Proceedings of the 25th Annual IEEE Applied Power Electronics Conference and Exposition (APEC 2010)*, 21–25 February 2010, pp. 2281–2287.
6. Colomer, J., Miribel-Catala, P., Saiz-Vela, A., & Samitier, J. (2010). A multi-harvested self-powered system in a low-voltage low-power technology. *IEEE Transactions on Industrial Electronics*, *58*(9), 4250–4263.
7. Lee, Y., Bang, S., Lee, I., Kim, Y., Kim, G., Ghaed, M. H., Pannuto, P., Dutta, P., Sylvester, D., & Blaauw, D. (2013). A modular 1 mm^3 die-stacked sensing platform with low power I^2C inter-die communication and multi-modal energy harvesting. *IEEE Journal of Solid-State Circuits*, *48*(1), January 2013, pp. 229–243.
8. Moore, G. E. (1965). Cramming more componentes onto integrated circuits. *Electronics*, *38*(8).
9. Courtland, R. (2013). The end of the shrink. *IEEE Spectrum*, *50*(11), 26–29.

10. Carli, D., Brunelli, D., Bertozzi, D., & Benini, L. (2010). A high-efficiency wind-flow energy harvester using micro turbine. In *Proceedings of the International Symposium on Power Electronics Electrical Drives Automation and Motion (SPEEDAM)*, 14–16 June 2010, pp. 778–783.
11. Trapanese, M. (2008). Optimization of a sea wave energy harvesting electromagnetic device. *IEEE Transactions on Magnetics*, *44*(11), 4365–4368.
12. Ramadass, Y. K., & Chandrakasan, A. P. (2010). An efficient piezoelectric energy harvesting interface circuit using a bias-flip rectifier and shared inductor. *IEEE Journal of Solid-State Circuits*, *45*(1), 189–204.
13. Dallago, E., Danioni, A., Marchesi, M., Nucita, V., & Venchi, G. (2011). A self-powered electronic interface for electromagnetic energy harvester. *IEEE Transactions on Power Electronics*, *26*(11), 3174–3182.
14. Kong, N., & Ha, D. S. (2012). Low-power design of a self-powered piezoelectric energy harvesting system with maximum power point tracking. *IEEE Transactions on Power Electronics*, *27*(5), 2298–2308.
15. Torres, E. O., & Rincón-Mora, G. A. (2009). Electrostatic energy-harvesting and battery-charging CMOS system prototype. *IEEE Transactions on Circuits and Systems I: Regular Papers*, *56*(9), 1938–1948.
16. Kumar, S. S., & Kashwan, K. R. (2013). Research study of energy harvesting in wireless sensor networks. *International Journal of Renewable Energy Research (IJRER)*, *3*(3), 745–753.
17. Paradiso, J. A., & Starner, T. (2005). Energy scavenging for mobile and wireless electronics. *IEEE Pervasive Computing, 4*(1), 18–27.
18. Rabaey, J., Burghardt, F., Steingart, D., Seeman, M., & Wright, P. (2007). Energy harvesting—a systems perspective. In *Proceedings of IEEE International Electron Devices Meeting (IEDM 2007)*, 10–12 December 2007, pp. 363–366.
19. Roundy, S., Wright, P., & Rabaey, J. (2003). *Energy scavenging for wireless sensor networks with special focus on vibrations*. Boston: Kluwer Academic Press.
20. Meninger, S., Mur-Miranda, J., Amirtharajah, R., Chandrakasan, A., & Lang, J. (2001). Vibration-to-electric energy conversion. *IEEE Transactions on Very Large Scale Integration (VLSI) Systems*, *9*(1), 64–76.
21. Lu, X., Yang, S.-H. (2010). Thermal energy harvesting for WSNs. In *Proceedings of the IEEE International Conference on Systems Man and Cybernetics (SMC 2010)*, 10–13 October 2010, pp. 3045–3052.
22. Becker, T., Kluge, M., Schalk, J., Otterpohl, T., & Hilleringmann, U. (2008). Power management for thermal energy harvesting in aircrafts. In *Proceedings of the IEEE Sensors 2008 Conference*, 26–29 October 2008, pp. 681–684.
23. Richelli, A., Colalongo, L., Tonoli, S., & Kovacs-Vajna, Z. M. (2009). A 0.2—1.2 V DC/DC boost converter for power harvesting applications. *IEEE Transactions on Power Electronics*, *24*(6), 1541–1546.
24. Lim, J., Huang, C.-K., Ryan, M., Snyder, G. J., Herman, J., & Fleurial, J.-P. (2008). MEMS/ECD method for making $Bi_{2-x}Sb_xTe_3$ thermoelectric devices. *NASA Tech Briefs*, *32*(7), NPO-30797.
25. Vadus, J. R. (2004). Some basic needs and concepts for 2020. In *Proceedings of the Oceans'04 MTTS/IEEE Techno-Ocean'04*, 9–12 November 2004, Vol. 1, p. 1.
26. Monfray, S., Puscasu, O., Savelli, G., Soupremanien, U., Ollier, E., Guerin, C., Frechette, L. G., Leveille, E., Mirshekari, G., Maitre, C., Coronel, P., Domanski, K., Grabiec, P., Ancey, P., Guyomar, D., Bottarel, V., Ricotti, G., Boeuf, F., Gaillard, F., & Skotnicki, T. (2012). Innovative thermal energy harvesting for zero power electronics. In *Proceedings of the IEEE Silicon Nanoelectronics Workshop (SNW 2012)*, 10–11 June 2012, pp. 1–4.
27. Ravindran, S. K .T., Nilkund, P., Kroener, M., & Woias, P. (2013). Thermal energy harvesting using an electrostatic generator. In *Proceedings of the IEEE 26th International Conference on Micro Electro Mechanical Systems (MEMS 2013)*, 20–24 January 2013, pp. 801–804.

28. Fernandes, J. R., Martins, M., & Piedade, M. (2010). An energy harvesting circuit for self-powered sensors. In *Proceedings of the 17th International Conference on Mixed Design of Integrated Circuits and Systems (MIXDES)*, 24–26 June 2010, pp. 205–208.
29. Gonçalves, H., Martins, M., & Fernandes, J. (2012). A study on MOSFET rectifiers with transistors operating in the weak inversion region. In *Proceedings of the 19th IEEE International Conference on Electronics, Circuits and Systems (ICECS 2012)*, 9–12 December 2012, pp. 665–668.
30. Visser, H. J., Reniers, A. C. F., Theeuwes, J. A. C. (2008). Ambient RF energy scavenging: GSM and WLAN power density measurements. In *Proceedings of the 38th European Microwave Conference (EuMC 2008)*, 27–31 October 2008, pp. 721–724.
31. Tucker, C. A., Warwick, K., & Holderbaum, W. (2013). A contribution to the wireless transmission of power. *International Journal of Electrical Power and Energy Systems*, *47*, 235–242.
32. Mikeka, C., Arai, H., Georgiadis, A., & Collado, A. (2011). DTV band micropower RF energy-harvesting circuit architecture and performance analysis. In *Proceedings of the IEEE International Conference on RFID-Technologies and Applications (RFID-TA 2011)*, 15–16 September 2011, pp. 561–567.
33. Parks, A. N., Sample, A. P., Zhao, Y., & Smith, J. R. (2013). A wireless sensing platform utilizing ambient RF energy. In *Proceedings of the IEEE Radio and Wireless Symposium (RWS 2013)*, 20–23 January 2013, pp. 331–333.
34. Mikeka, C., & Arai, H. (2011). Dual-band RF energy-harvesting circuit for range enhancement in passive tags. In *Proceedings of the 5th European Conference on Antennas and Propagation (EUCAP)*, 11–15 April 2011, pp. 1210–1214.
35. Kim, J., Nam, C., & Lee, K.-Y. (2010). A design of transceiver for 13.56 MHz RFID reader using the peak detector with automatic reference voltage generator and voltage limiter. In *Proceedings of the International SoC Design Conference (ISOCC 2010)*, 22–23 November 2010, pp. 287–289.
36. Fernandez, E., Beriain, A., Solar, H., Garcia-Alonso, A., Berenguer, R., Sosa, J., Monzon, J. M., Garcia-Alonso, S., & Montiel-Nelson, J. A. (2011). Low power voltage limiter design for a full passive UHF RFID sensor. In *Proceedings of the IEEE 54th International Midwest Symposium on Circuits and Systems (MWSCAS 2011)*, 7–10 August 2011, pp. 1–4.
37. Starner, T. (1996). Human-powered wearable computing. *IBM Systems Journal, 35*(3 & 4), 618–629.
38. Zeng, P., Chen, H., Yang, Z., & Khaligh, A. (2011). Unconventional wearable energy harvesting from human horizontal foot motion. In *Proceedings of the 26th Annual IEEE Applied Power Electronics Conference and Exposition (APEC 2011)*, 6–11 March 2011, pp. 258–264.
39. Hayakawa, M. (1991). *Electric wristwatch with generator*. U.S. Patent 5 001 685, March 1991.
40. Mitcheson, P. D. (2010). Energy harvesting for human wearable and implantable bio-sensors. In *Proceedings of the Annual International Conference of the IEEE Engineering in Medicine and Biology Society (EMBC 2010)*, 31 August 2010–4 September 2010, pp. 3432–3436.
41. Hoang, D. C., Tan, Y. K., Chng, H. B., & Panda, S. K. (2009). Thermal energy harvesting from human warmth for wireless body area network in medical healthcare system. In *Proceedings of the International Conference on Power Electronics and Drive Systems (PEDS 2009)*, 2–5 November 2009, pp. 1277–1282.
42. Shahhaidar, E., Boric-Lubecke, O., Ghorbani, R., & Wolfe, M. (2011). Electromagnetic generator: As respiratory effort energy harvester. In *Proceedings of the IEEE Power and Energy Conference at Illinois (PECI 2011)*, 25–26 February 2011, pp. 1–4.
43. Paulides, J. J. H., Jansen, J. W., Encica, L., Lomonova, E. A., & Smit, M. (2011). Power from the people. *IEEE Industry Applications Magazine, 17*(5), 20–26.
44. Elvin, N. G., & Elvin, A. A. (2013). Vibrational energy harvesting from human gait. *IEEE/ASME Transactions on Mechatronics*, *18*(2), 637–644.

45. Luciano, V., Sardini, E., Serpelloni, M., & Baronio, G. (2012). Analysis of an electromechanical generator implanted in a human total knee prosthesis. In *Proceedings of the IEEE Sensors Applications Symposium (SAS 2012)*, 7–9 February 2012, pp. 1–5.
46. Tsai, J., Wang, J., & Su, Y. (2013). Piezoelectric rubber films for human physiological monitoring and energy harvesting. In *Proceedings of the IEEE 26th International Conference on Micro Electro Mechanical Systems (MEMS 2013)*, 20–24 January 2013, pp. 841–844.
47. Hwang, J. H., Kang, T. W., Hyoung, C. H., & Kang, S. W. (2012). Receptive properties of the human body of emitted electromagnetic waves for energy harvesting. In *IEEE International Symposium on Antennas and Propagation Society (APSURSI 2012)*, 8–14 July 2012, pp. 1–2.
48. Hwang, J. H., Hyoung, C. H., Park, K. H., & Kim, Y. T. (2013). Energy harvesting from ambient electromagnetic wave using human body as antenna. *Electronics Letters*, *49*(2), 17 January 2013, pp. 149–151.
49. Meehan, A., Gao, H., & Lewandowski, Z. (2011). Energy harvesting with microbial fuel cell and power management system. *IEEE Transactions on Power Electronics*, *26*(1), January 2011, pp. 176–181.
50. Chen, Y., Twigg, C. M., Sadik, O. A., & Tong, S. (2011). A self-powered adaptive wireless sensor network for wastewater treatment plants. In *IEEE International Conference on Pervasive Computing and Communications Workshops (PERCOM Workshops 2011)*, 21–25 March 2011, pp. 356–359.
51. Park, J.-D., & Ren, Z. (2011). Efficient energy harvester for microbial fuel cells using DC/DC converters. In *Proceedings of the IEEE Energy Conversion Congress and Exposition (ECCE 2011)*, 17–22 September 2011, pp. 3852–3858.
52. Kung, C.-C., Liu, C.-C., Sun, Y., & Yu, X. (2012). Innovative Microbial Fuel cell for energy harvesting. In *Proceedings of the IEEE Energytech 2012*, 29–31 May 2012, pp. 1–4.
53. Chen, C. J. (2011). *Physics of solar energy*. Hoboken: Wiley.
54. Šúri M., Huld T. A., Dunlop E. D., & Ossenbrink H. A. (2007). Potential of solar electricity generation in the European Union member states and candidate countries. *Solar Energy*, *81*, 1295–1305. Available http://re.jrc.ec.europa.eu/pvgis/
55. Huld, T., Müller, R., & Gambardella, A. (2012). A new solar radiation database for estimating PV performance in Europe and Africa. *Solar Energy, 86*, 1803–1815.
56. Randall, J. F., & Jacot, J. (2003). Is AM1.5 applicable in practice? Modelling eight photovoltaic materials with respect to light intensity and two spectra. *Renewable Energy*, *28*(12), 1851–1864.
57. Weddel, A. S., Merret, G. V., & Al-Hashimi, B. M. (2012). Photovoltaic sample-and-hold circuit enabling MPPT indoors for low-power systems. *IEEE Transactions on Circuits and Systems I: Regular Papers*, *59*(6), pp. 1196–1204.
58. Hande, A., Polk, T., Walker, W., & Bhatia, D. (2007). Indoor solar energy harvesting for sensor network router nodes. *Microprocessors and Microsystems*, *31*(6), 420–432.
59. Nasiri, A., Zabalawi, S. A., & Mandic, G. (2009). Indoor power harvesting using photovoltaic cells for low-power applications. *IEEE Transactions on Industrial Electronics*, *56*(11), 4502–4509.
60. Javanmard, N., Vafadar, G., & Nasiri, A. (2009). Indoor power harvesting using photovoltaic cells for low power applications. In *Proceedings of the 13th European Conference on Power Electronics and Applications (EPE'09)*, 8–10 September 2009, pp. 1–10.
61. Wang, W. S., O'Donnell, T., Wang, N., Hayes, M., O'Flynn, B., & O'Mathuna, C. (2010). Design considerations of sub-mW indoor light energy harvesting for wireless sensor systems. *ACM Journal on Emerging Technologies in Computing Systems (JETC)*, *6*(2), article 6.
62. Dondi, D., Bertacchini, A., Larcher, L., Pavan, P., Brunelli, D., & Benini, L. (2008). A solar energy harvesting circuit for low power applications. In *Proceedings of the IEEE International Conference on Sustainable Energy Technologies (ICSET 2008)*, 24–27 November 2008, pp. 945–949.
63. Jeong, J., Jiang, X., & Culler, D. (2008). Design and analysis of micro-solar power systems for wireless sensor networks. In *Proceedings of the 5th International Conference on Networked Sensing Systems (INSS 2008)*, 17–19 June 2008, pp. 181–188.

64. Sharma, N., Gummeson, J., Irwin, D., & Shenoy, P. (2010). Cloudy Computing: Leveraging Weather Forecasts in Energy Harvesting Sensor Systems. In *Proceedings of the 7th Annual IEEE Communications Society Conference on Sensor Mesh and Ad Hoc Communications and Networks (SECON 2010)*, 21–25 June 2010, pp. 1–9.
65. Lee, J. S., Hornsey, R. I., & Renshaw, D. (2003). Analysis of CMOS Photodiodes I—Quantum efficiency. *IEEE Transactions on Electron Devices*, *50*(5), pp. 1233–1238.
66. Lee, J. S., Hornsey, R. I., & Renshaw, D. (2003). Analysis of CMOS photodiodes II—lateral photoresponse. *IEEE Transactions on Electron Devices*, *50*(5), pp. 1239–1245.
67. Esram, T., & Chapman, P. L. (2007). Comparison of Photovoltaic Array Maximum Power Point Tracking Techniques. *IEEE Transactions on Energy Conversion*, *22*(2), 439–449.
68. Guilar, N. J., Kleeburg, T. J., Chen, A., Yankelevich, D. R., & Amirtharajah, R. (2009). Integrated solar energy harvesting and storage. *IEEE Transactions on Very Large Scale Integration (VLSI) Systems*, *17*(5), 627–637.
69. Guilar, N. J., Fong, E. G., Kleeburg, T., Yankelevich, D. R., & Amirtharajah, R. (2008). Energy harvesting photodiodes with integrated 2D diffractive storage capacitance. In *Proceedings of the ACM/IEEE International Symposium on Low Power Electronics and Design (ISLPED)*, 11–13 August 2008, pp. 63–68.
70. Ferri, M., Pinna, D., Dallago, E., & Malcovati, P. (2009). A 0.35 μm CMOS Solar energy scavenger with power storage management system. In *Proceedings of the Ph.D. Research in Microelectronics and Electronics (PRIME 2009)*, 12–17 July 2009, pp. 88–91.
71. Ferri, M., Pinna, D., Malcovati, P., Dallago, E., & Ricotti, G. (2009). Integrated stabilized photovoltaic energy harvester. In *Proceedings of the 16th IEEE International Conference on Electronics, Circuits and Systems (ICECS 2009)*, 13–16 December 2009, pp. 299–302.
72. Barnett, A., Honsberg, C., Kirkpatrick, D., Kurtz, S., Moore, D., Salzman, D., Schwartz, R., Gray, J., Bowden, S., Goossen, K., Haney, M., Aiken, D., Wanlass, M., & Emery, K. (2006). 50 % efficient solar cell architectures and designs. In *Conference records of the IEEE 4th World Conference on Photovoltaic Energy Conversion*, May 2006, Vol. 2, pp. 2560–2564.
73. Amaral, A., Lavareda, G., Carvalho, C. N., Brogueira, P., Gordo, P. M., Subrahmanyam, V. S., Gil, C. L., Naia, V. D., & Lima, A. P. (2002). Influence of the a-Si:H structural defects studied by positron annihilation on the solar cells characteristics. *Thin Solid Films*, *403–404*, 539–542.
74. Ramanan, A. V., Pakirisamy, M., & Williamson, S. S. (2011). Photosynthetic electrochemical cell charging infrastructure versus photovoltaic cell charging infrastructure for future electric vehicles. In *Proceedings of the IEEE Vehicle Power and Propulsion Conference (VPPC 2011)*, 6–9 September 2011, pp. 1–5.
75. Sudevalayam, S., & Kulkarni, P. (2011). Energy harvesting sensor nodes: Survey and implications. *IEEE Communications Surveys and Tutorials, 13*(3), 443–461.
76. Kansal, A., Hsu, J., Zahedi, S., & Srivastava, M. B. (2007). Power management in energy harvesting sensor networks. *ACM Transactions on Embedded Computing Systems, 6*, 2007.
77. Vigorito, C. M., Ganesan, D., & Barto, A. G. (2007). Adaptive control of duty cycling in energy-harvesting wireless sensor networks. In *Proceedings of the 4th Annual IEEE Communications Society Conference on Sensor, Mesh and Ad Hoc Communications and Networks (SECON 2007)*, 18–21 June 2007, pp. 21–30.
78. Sun, Z.-J., Li, W.-B., Xiao, H.-F., & Xu, L. (2010). The Research on Solar Power System of Wireless Sensor Network Node for Forest Monitoring. In *Proceedings of the International Conference on Web Information Systems and Mining (WISM 2010)*, 23–24 October 2010, Vol. 2, pp. 395–398.
79. Wang, W., Wang, N., Jafer, E., Hayes, M., O'Flynn, B., & O'Mathuna, C. (2010). Autonomous wireless sensor network based building energy and environment monitoring system design. In *Proceedings of the 2nd Conference on Environmental Science and Information Application Technology (ESIAT)*, 17–18 July 2010, pp. 367–372.
80. Thewes, M., Scholl, G., & Li, X. (2012). Wireless energy autonomous sensor networks for automobile safety systems. In *Proceedings of the 9th International Multi-Conference on Systems, Signals and Devices (SSD 2012)*, 20–23 March 2012, pp. 1–5.

81. Park, G., Rosing, T., Todd, M., Farrar, C., & Hodgkiss, W. (2008). Energy Harvesting for Structural Health Monitoring Sensor Networks. *Journal of Infrastructure Systems*, *14*(1), 64–79.
82. Gutiérrez, A., Dopico, N. I., Gonzalez, C., Zazo, S., Jimenez-Leube, J., & Raos, I. (2013). Cattle-Powered Node Experience in a Heterogeneous Network for Localization of Herds. *IEEE Transactions on Industrial Electronics*, *60*(8), 3176–3184.
83. Wang, W. S., O'Donnell, T., Ribetto, L., O'Flynn, B., Hayes, M., & O'Mathuna, C. (2009). Energy harvesting embedded wireless sensor system for building environment applications. In *Proceedings of the 1st International Conference on Wireless Communication, Vehicular Technology, Information Theory and Aerospace and Electronic Systems Technology (Wireless VITAE 2009)*, 17–20 May 2009, pp. 36–41.

http://www.springer.com/978-3-319-21616-4

CMOS Indoor Light Energy Harvesting System for Wireless Sensing Applications

Ferreira Carvalho, C.M.; Paulino, N.

2016, XIV, 216 p. 145 illus., 74 illus. in color., Hardcover
ISBN: 978-3-319-21616-4